Processing and Application of Ceramics 12 [3] (2018) 262–267
https://doi.org/10.2298/PAC1803262R

The luminescence properties of yttria based phosphors and study of YBO_3 formation via H_3BO_3 addition

Seyed Mahdi Rafiaei*

Department of Materials Science and Engineering, Golpayegan University of Technology, Golpayegan, Isfahan, Iran

Received 26 April 2018; Received in revised form 31 July 2018; Accepted 20 August 2017

Abstract

In this paper, Y_2O_3:Eu^{3+} nano-phosphor was synthesized through the facile solid-state method and influence of H_3BO_3 addition to the prepared Y_2O_3:Eu^{3+} powder was investigated. The consumption of boric acid resulted in the formation of YBO_3 by changing the crystal structure from cubic to hexagonal. Noteworthy, through the use of specific quantities of H_3BO_3 (medium amount), Y_3BO_6 impurity with the monoclinic crystal structure and the space group C2/m was formed. FESEM observations showed that the addition of H_3BO_3 leads to the coarsening of the synthesized particles; changing from approximately 80 nm to 1 μm. Also, it was concluded that the transformation of the crystal structure causes a dramatic change of phosphor emission colours from reddish to orange.

Keywords: *Y_2O_3:Eu^{3+}, YBO_3 formation, structure, luminescence properties*

I. Introduction

Eu^{3+} doped Y_2O_3 and YBO_3 phosphors with brilliant emission characteristics and significant chemical stability have received much attention of researchers and engineers for their potential applications in optics-related fields [1,2]. Yttria is widely used in various interesting applications, such as white light emitting diodes [3], photovoltaic cells, up-conversion phosphors [4], lighting, sensors, and optical amplifiers [5]. Meanwhile, the main applications of YBO_3 are display panels, the next generation of flexible display instruments and LEDs [6,7]. Surprisingly, YBO_3 phosphor can be synthesized easily through the addition of boric acid to $Y(CH_3COO)_3 \cdot xH_2O$, but the crystal structure and luminescence characteristics of these two oxides are absolutely different. Y_2O_3 phosphors possess cubic crystal structure and *Ia*3 space group (No. 206). It is already known that in the crystal structure of Y_2O_3 host lattice, two types of trivalent yttrium ions can be found. Three-quarters of these locations are non-centrosymmetric with *C*2 symmetry and the rest one quarter is centrosymmetric with *S*6 symmetry. It should be noted that YBO_3 compound crystallizes in different structures with different space groups and symmetries [8,9]. In the monoclinic YBO_3 host lattice, two kinds of Y^{3+} ions with *C*1 and *Ci* crystal symmetries have been reported [7]. Furthermore, YBO_3 may have a hexagonal crystal structure with a *P*63/*m* space group (No. 176) and Eu^{3+} ions which are substituted into Y^{3+} sites, have been surrounded by BO_3 groups. So, they provide a symmetry centre resulting in a strong $^5D_0 - ^7F_1$ transition [10].

The extensive studies about Y_2O_3 reveal that different methods have been used to synthesize it, e.g. hydrothermal [11,12], sol-gel [13], spray pyrolysis [14], combustion [15,16], co-precipitation [17], micro-emulsion microwave [18] and electrospinning [19]. In addition, YBO_3 has been extensively synthesized through the employment of the wide range of techniques, such as combustion [20], solvothermal [21], solid-state [10], sol-gel [22], spray pyrolysis [23] and hydrothermal [24]. From the described approaches, plenty of research works have been devoted to the investigation of the facile, economic and effective solid-state procedure. However, the critical problem in the synthesis of the YBO_3 phosphor is that H_3BO_3 with a relatively low boiling temperature is not stable during application of high temperatures. So, large amounts of H_3BO_3 are subjected to evaporation and estimating the required quantities of boric acid to

*Corresponding authors: tel: +98 91 3139 0739,
e-mail: *rafiaei@gut.ac.ir*

produce YBO_3 is complicated in a way. Also, the addition of boric acid may give rise to the formation of impurities. Unfortunately, the literature is scarce on these issues and this work can provide important information about the optimum values of H_3BO_3 quantities for the synthesis of YBO_3.

Motivated by this brief background and the lack of the related database, the Y_2O_3 phosphor was synthesized via the simple solid-state technique. Transformation from Y_2O_3 to YBO_3 host lattice by addition of H_3BO_3 was investigated by XRD and FESEM. The luminescence studies on Eu^{3+} doped Y_2O_3 and YBO_3 phosphor materials were also carried out.

II. Experimental

2.1. Preparation

In this work, $(Y_{0.96}Eu_{0.04})_2O_3$ phosphor was synthesized through the use of yttrium acetate ($Y(CH_3COO)_3 \cdot xH_2O$) and europium oxide (Eu_2O_3). The precursor powders with the highest purity (99.99%) were purchased from Aldrich Company and consumed without any purification. Accordingly, stoichiometric amounts of $Y(CH_3COO)_3 \cdot xH_2O$ and Eu_2O_3 were ground in a crucible. Then, this mixture was transferred to a tube furnace to conduct calcination at 1100 °C for 2 h. The phosphors nominated as P_0, $P_{0.02}$, $P_{0.05}$, $P_{0.15}$, $P_{0.25}$, $P_{0.5}$, P_1, P_2, and P_4 (see Table 1) were synthesized through consuming specific amounts of H_3BO_3, i.e. required amounts of boric acid were added to the calcined initial materials, followed by grinding.

Table 1. Sample notation and corresponding ratio of consumed H_3BO_3 to its stoichiometric quantity (R)

Sample notation	R
P_0	0
$P_{0.02}$	0.02
$P_{0.05}$	0.05
$P_{0.15}$	0.15
$P_{0.25}$	0.25
$P_{0.5}$	0.5
P_1	1
P_2	2
P_4	4

2.2. Characterization

To identify the crystal structure of the synthesized phosphors, X-ray diffraction (XRD, Rigaku, Japan) with CuKα radiation (λ = 1.54 Å) was employed. The Scherrer formula, $D = 0.9\lambda/\beta\cos\theta$, was used to estimate the crystallite size of the prepared samples (where D is the average grain size, λ is the wavelength of X-ray, β and θ are the full-width at half maximum and diffraction angle of the considered peaks, respectively). In addition, the morphology of produced phosphors was studied via the use of field emission scanning electron microscope (FE-SEM, Hitachi SU70, Japan). Finally, the optical properties of Y_2O_3/YBO_3 phosphors were characterized by a photoluminescence analyser (PL, Horiba Jobin Yvon Fluorolog-3, Japan).

III. Results and discussion

3.1. XRD analysis

Figure 1 shows the XRD spectra of P_0-P_4 compounds. The spectra of P_0-$P_{0.15}$ compounds imply that the prominent peaks of diffraction are attributed to (211), (222), (400), (440) and (622) planes of a cubic crystal structure, suggesting that the obtained phosphor matches well with JCPDS No. 41-1105. Also, regarding the Scherrer formula, the crystallite size of Y_2O_3 (P_0) phosphor was simply calculated to be 45.6 nm. Accordingly, it is clear that for R values from 0 to 0.25, the structure of the synthesized phosphors is very similar to that of Y_2O_3. Obviously, the peak at 29.2° of (222) plane has the strongest intensity of diffraction, while the addition of small quantities of boric acid gives rise to its slight increase. Conversely, the use of higher quantities of the additive significantly decreases the diffraction intensity, thus suppresses the crystallization of Y_2O_3.

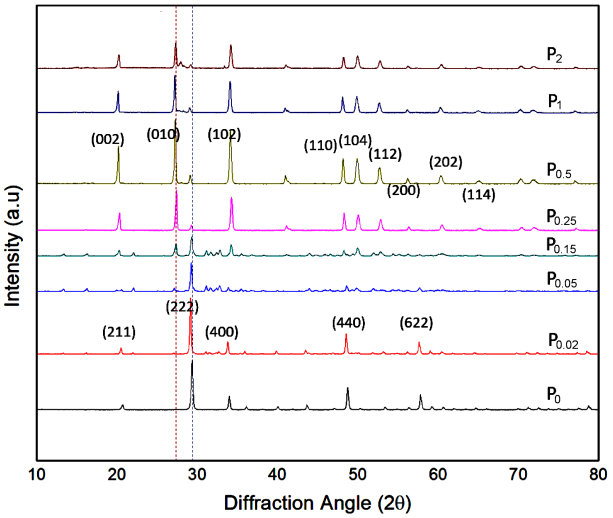

Figure 1. XRD spectra of P_0-P_2 phosphor compounds

As a matter of fact, boric acid has the role of flux material via the solid-state procedure. With the use of small amounts of the additive, the crystallinity of the synthesized phosphor is improved. This issue is related to the fact that the mentioned material, with a relatively lower melting point, facilitates the melting of components and enhances the growth of yttria crystals [10]. In other words, according to our calculations, it was found that the addition of small amounts of H_3BO_3, has enlarged the distance of (222) plane from 3.035 Å to 3.059 Å, implying the expansion of yttria unit cell. However, higher amounts of H_3BO_3, not only decreases the peak intensity but also shrinks the inter-planar distance from 3.059 Å to 3.053 Å and 3.052 Å. This observation clarifies that relatively larger amounts of the used additive suppress the growth of Y_2O_3 material. It seems that the flux material provides efficient obstacles among

the produced oxide nano-particles. The study of XRD spectra of $P_{0.25}$-P_2 compounds shows that the synthesized phosphors belong to YBO_3 phase, possess hexagonal crystal structure and are consistent with JCPDS No. 16-0277. The prominent diffraction peaks are attributed to (002), (010), (102), (110), (104), (112), (200), (202), and (114) planes. Interestingly, by the addition of boric acid the prominent peak of the considered compounds shifts from approximately 29.2° to 27.26° (shown by the dashed lines). The XRD spectra of $P_{0.5}$, P_1, and P_2 phosphors reveal that further increase of H_3BO_3 leads to the significant formation of YBO_3. Consequently, exploring the probable reactions within the solid-state procedure remains an interesting issue in this study. The possible reactions between Y_2O_3 and H_3BO_3 can be considered as follows:

$$Y_2O_3 + 2\,H_3BO_3 \rightleftharpoons 2\,YBO_3 + 3\,H_2O \quad (1)$$

$$2\,Y_2O_3 + 2\,H_3BO_3 \rightleftharpoons YBO_3 + Y_3BO_6 + 3\,H_2O \quad (2)$$

It can be easily found that with the addition of H_3BO_3 during the explained solid-state procedure, YBO_3 or YBO_3/Y_3BO_6 can be produced. Therefore, the formation of Y_3BO_6 was monitored by the employment of XRD spectra. As a matter of fact, in the case of using large amounts of boric acid, especially for synthesis of P_2 phosphor, some impurity peaks can be seen. Referring to the mentioned reactions and also JCPDS No. 34-0291, 41-1105 and 16-0277, it can be easily concluded that the impurity peaks include Y_2O_3 and Y_3BO_6 phases.

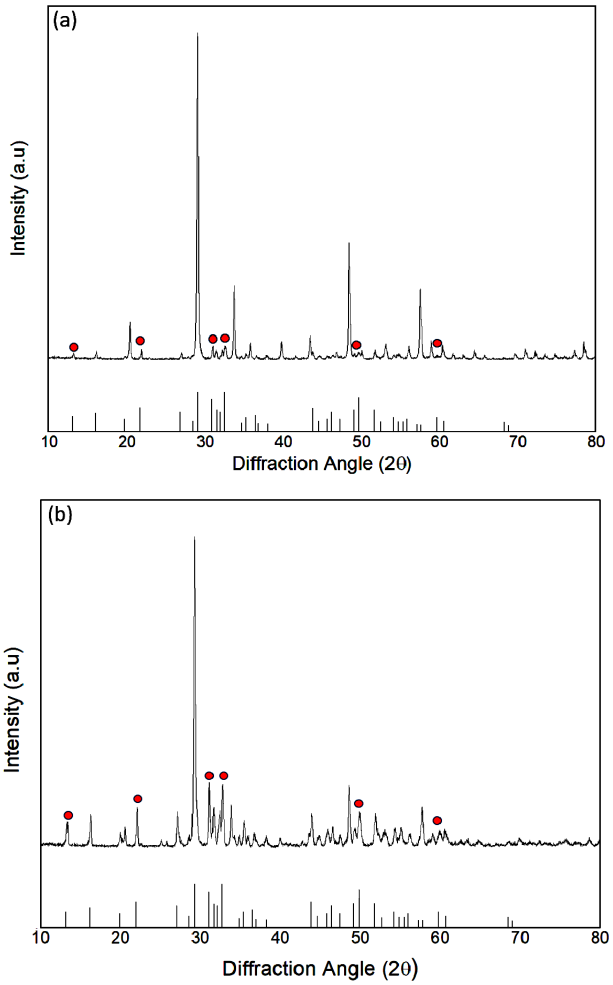

Figure 2. XRD spectra of: a) $P_{0.15}$ and b) $P_{0.25}$ phosphors

Figure 2 shows the existence of Y_3BO_6 impurities in $P_{0.15}$ and $P_{0.25}$ phosphors marked with the red circles. It is seen that the attributed main diffraction planes can be seen at the 2θ of 13.34°, 22.06°, 31.11°, 32.75°, 49.95° and 59.73°. It is obviously observed that the increase of boric acid addresses the increase of considered diffraction intensities. Y_3BO_6 crystallizes in the monoclinic space group $C2/m$, with the lattice constants: a = 18.162 Å, b = 3.651 Å and c = 14.006 Å, while α, β and γ are 90°, 119.69° and 90°, respectively (JCPDS No. 34-0291). It is clear that the formation of Y_3BO_6 is achieved for the specific amounts of H_3BO_3 which is in agreement with the introduced solid-state reactions. It can be seen that the strongest diffraction intensities belong to $P_{0.15}$ and $P_{0.25}$ materials.

3.2. *FESEM observations*

According to Figure 3, it is seen that the particle size of P_0 sample is about 80 nm, while through the addition of boric acid, the particle size grows gradually to approximately 1 μm in P_2 phosphor. Interestingly with the increase of H_3BO_3, the particle size changed dramatically from nanoscale to microscale. This result is consistent with the crystallite sizes of P_0 and P_2 phosphors, which were estimated to 45.6 nm and 52.4 nm, respectively. In other words, it is observed that with the use of boric acid via solid-state approach, the transformation of materials from Y_2O_3 to YBO_3 with a huge growth of particles would happen.

3.3. *PL analysis*

The excitation characterization was conducted on $P_{0.02}$ compound (see Fig. 4a), since according to the discussed XRD spectra, $P_{0.02}$ phosphor possesses well-formed crystal structure. There is a broad band from 210 nm to 280 nm that is attributed to the charge transfer band (CTB) between O^{2-} and Eu^{3+} ions with the orbitals of $2p$ and $4f$, respectively [25]. Figure 4b belongs to the photoluminescence emission of P_0 and $P_{0.5}$ compounds under the excitation wavelength of 255 nm. The PL spectrum of P_0 sample is composed of $^5D_0-^7F_1$ and $^5D_0-^7F_2$ peaks which are related to the magnetic dipole and forced electric dipole transitions. It can be easily found that $^5D_0-^7F_2$ is the dominant peak observed at 612 nm [26]. Usually in the cubic crystal structure of Y_2O_3, through the substitution of Y^{3+} by Eu^{3+} ions, no inversion centre is provided and the electric dipole transition is partially allowed. Furthermore, the $^5D_0-^7F_1$ and $^5D_0-^7F_2$ transitions are observed in the emission result of $P_{0.5}$ sample too. By contrast, it is seen that the $^5D_0-^7F_1$ magnetic dipole transition at 592 nm

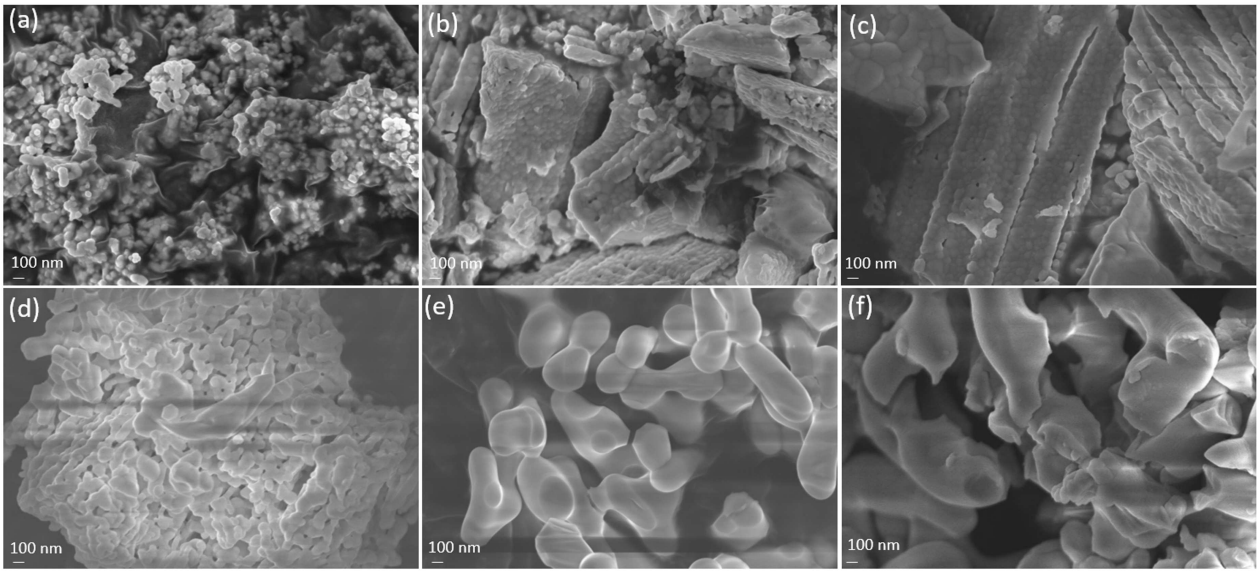

Figure 3. FESEM images of: a) P_0, b) $P_{0.05}$, c) $P_{0.15}$, d) $P_{0.25}$, e) $P_{0.5}$ and f) P_2 luminescent compounds

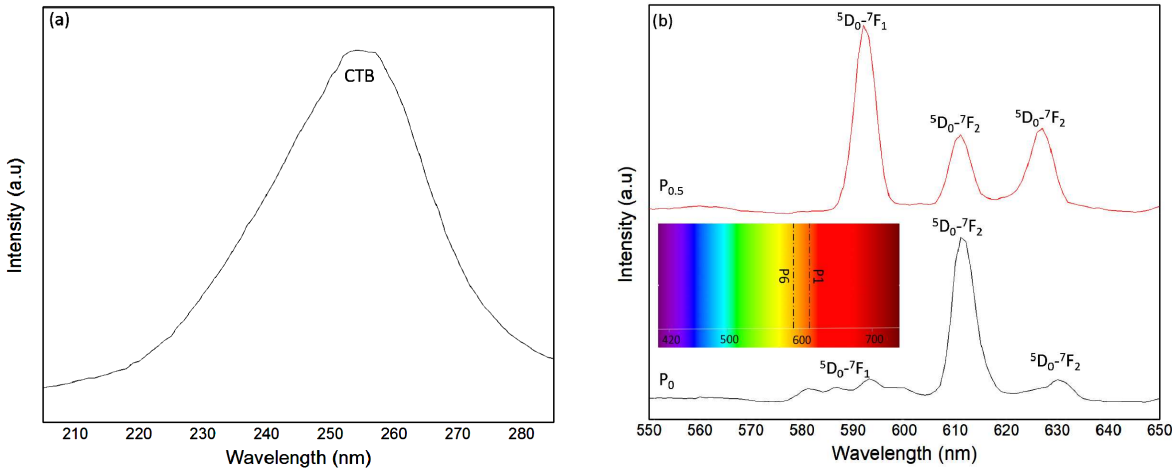

Figure 4. Photoluminescence: a) excitation spectrum of $P_{0.02}$ and b) emission spectra of P_0, $P_{0.5}$ phosphors

is the dominant peak [25]. YBO_3 host lattice possesses a hexagonal crystal structure in which Y^{3+} ions are surrounded by BO_3 groups. Through the doping procedure, the ions of Eu^{3+} are substituted at Y sites, making a symmetry centre and also a powerful $^5D_0-^7F_1$ transition occurs. Noteworthy, with the increase of boric acid and the transformation of the crystal structure from cubic to hexagonal, the emission colour of produced phosphors changes slightly from reddish to orange (see the inset of Fig. 4b).

Figure 5a shows the emission behaviour of P_0-$P_{0.15}$ phosphors. It is concluded that the addition of small amounts of H_3BO_3 to yttrium acetate within the solid-state process, improves the photoluminescence properties, effectively. Interestingly, this result agrees well with the XRD spectra and clarifies that the addition of H_3BO_3 has enhanced the crystallinity of Y_2O_3 host lattice. However, similar to the results reported by other researchers, it is clear that higher quantities of the flux decrease the luminescence properties of phosphors [27,28]. Noteworthy, in this case, the additives give rise to the formation of impurities, suppress the crystallinity and therefore photoluminescence characteristics of the synthesized phosphors. According to Fig. 5b, it is observed that the highest and the lowest intensities of PL spectra of YBO_3 based phosphors are attributed to $P_{0.5}$ and P_2 compounds, respectively. It can be mentioned that based on the low boiling point of H_3BO_3, there is a remarkable evaporation of boric acid within the high temperature solid-state procedure. Therefore, $P_{0.5}$ sample has higher luminescence properties than $P_{0.25}$ phosphor. However, if the quantity of added boric acid is more than the required mass for the formation of YBO_3, some impurities will be made in the compound and thus the intensity of photoluminescence emission would be suppressed.

Interestingly, although Y_3BO_6 was detected in XRD spectra, no specific emission peak was observed related to the considered Y_3BO_6. The volumes of Y_2O_3 and Y_3BO_6 unit cells are 1192.4 Å^3 and 806.80 Å^3, respec-

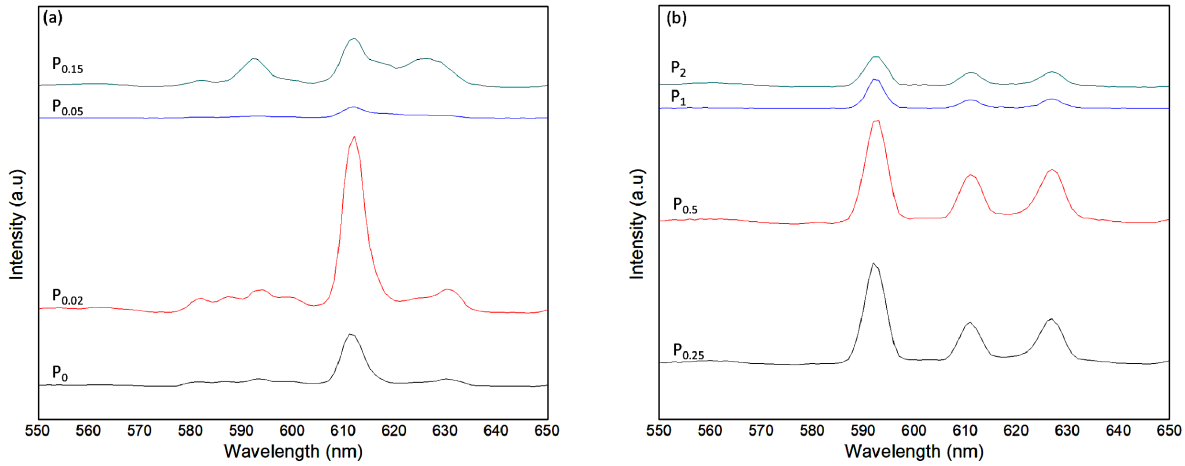

Figure 5. Photoluminescence emission of (a) P_0-$P_{0.15}$ and (b) $P_{0.25}$-P_2 phosphors

tively, which results in the larger distance of Y–O in Y_2O_3 than that in Y_3BO_6. Regarding the ionic sizes of Y^{3+} and Eu^{3+}, which are 1.04 Å and 1.087 Å, respectively, it is easily found that Eu^{3+} ions prefer to be doped more efficiently in the Y_2O_3 host. Moreover, as shown in the XRD spectra, Y_3BO_6 has been formed as an impurity and the quantity of this compound is very small. So, any specified peak cannot be observed in the PL spectra.

IV. Conclusions

In this work, Eu^{3+} doped Y_2O_3 nano-phosphor and YBO_3 phosphor were synthesized via facile solid-state approach. It was found that the addition of H_3BO_3 not only increases the particle size from approximately 80 nm to 1 μm, but also changes the crystal structure from cubic to hexagonal (belonging to YBO_3). In addition, the XRD results showed that Y_3BO_6 (as an impurity phase) was formed with the addition of medium amount of boric acid. The luminescence analyses proved that $P_{0.02}$ and $P_{0.5}$ compounds show the highest emission intensity for the Y_2O_3 and YBO_3 based phosphors, respectively.

Acknowledgements: Hereby the supports of the Golpayegan University of Technology are appreciated.

References

1. A.P. Jadhav, A.U. Pawar, U. Pal, Y.S. Kang, "Red emitting Y_2O_3:Eu^{3+} nanophosphors with >80% down conversion efficiency", *J. Mater. Chem. C*, **2** (2014) 496–500.
2. X. Zhang, Y. Fu, Z. Zhao, J. Yang, N. Li, M. Zhang, "Statistical design for the optimization of the red to orange ratio in YBO_3:Eu^{3+} phosphors", *J. Lumin.*, **194** (2018) 311–315.
3. Q.L. Dai, M.E. Foley, C.J. Breshike, A. Lita, G.F. Strouse, "Ligand-passivated Eu:Y_2O_3 nanocrystals as a phosphor for white light emitting diodes", *J. Am. Chem. Soc.*, **133** (2011) 15475–15486.
4. X.P. Qin, G.H. Zhou, H. Yang, Y. Yang, J. Zhang, S.W. Wang, "Synthesis and upconversion luminescence of monodispersed, submicron-sized Er^{3+}:Y_2O_3 spherical phosphors", *J. Alloys Compd.*, **493** (2010) 672–677.
5. V. Singh, V.K. Rai, I. Ledoux-Rak, S. Watanabe, T.K. Gundu Rao, J. Chubaci, L. Badie, F. Pelle, S. Ivanova, "NIR to visible up-conversion, infrared luminescence, thermoluminescence and defect centres in Y_2O_3:Er phosphor", *J. Phys. D: Appl. Phys.*, **42** (2009) 065104.
6. L. Chen, X. Deng, S. Xue, A. Bahader, E. Zhao, Y. Mua, H. Tian, S. Lu, K. Yu, Y. Jiang, S. Chen, Y. Tao, W. Zhang, "The energy transfer in the Sb^{3+} and Eu^{3+} co-activated YBO_3 phosphor and their white luminescence for deep ultraviolet LEDs application", *J. Lumin.*, **149** (2014) 144–149.
7. R.G. Nair, S. Nigam, B. Vishwanadh, V. Sudarsan, R.K. Vatsa, C. Majumder, V.K. Jain, "Size induced modification of boron structural unit in YBO_3: Systematic investigation by experimental and theoretical methods", *RSC. Adv.*, **6** (2016) 64065–64071.
8. G.X. Gua, D. Wanga, X.S. Lva, S.M. Wana, J.L. Youb, Q.L. Zhanga, S.T. Yin, "In situ study on the structural transition in YBO_3 through Raman spectroscopy", *Mater. Chem. Phys.*, **131** (2011) 274–277.
9. K. Yano, S. Takeshita, Y. Iso, T. Isobe, "Combinatorial optimization of the atomic compositions for green-emitting YBO_3:Ce^{3+},Tb^{3+} and red-emitting YBO_3:Ce^{3+},Tb^{3+},Eu^{3+} phosphors using a microplate reader", *RSC. Adv.*, **7** (2017) 17586–17592.
10. S.M. Rafiaei, "Effect of flux compounds on the luminescence properties of Eu^{3+} doped YBO_3 phosphors", *Mater. Sci. Pol.*, **34** (2016) 780–785.
11. L. Gao, G. Wang, H. Zhu, W. Zhou, G. Ou, "Hydrothermal synthesis of Y_2O_3 coated Y_2O_3:Eu^{3+} nanotubes for enhanced photoluminescence properties", *Mater. Res. Bull.*, **70** (2015) 876–880.
12. L. Mancic, V. Lojpur, B.A. Marinkovic, M.D. Dramicanin, O. Milosevic, "Hydrothermal synthesis of nanostructured Y_2O_3 and $(Y_{0.75}Gd_{0.25})_2O_3$ based phosphors", *Opt. Mater.*, **35** (2013) 1817–1823.
13. R.M. Vazquez, M.G. Hernandez, A.L. Marure, P.Y.L. Camacho, A.D.J.M. Ramirez, H.I.B. Conde, "Sol-gel synthesis and antioxidant properties of yttrium oxide nanocrystallites incorporating P-123", *Materials*, **7** (2014) 6768–6778.

14. H.Y. Koo, S.H. Ju, S.K. Hong, D.S. Jung, Y.C. Kang, K.Y. Jung, "Effect of boric acid flux and drying control chemical additive on the characteristics of Y_2O_3:Eu phosphor particles prepared by spray pyrolysis", *Jpn. J. Appl. Phys.*, **45** (2006) 9083–9087.
15. S.M. Rafiaei, A. Kim, M. Shokouhimehr, "Enhanced luminescence properties of combustion synthesized Y_2O_3:Gd nanostructure", *Current. Nanosci.*, **12** (2016) 244–249.
16. M. Shokouhimehr, S.M. Rafiaei, "Combustion synthesized YVO_4:Eu^{3+} phosphors: effect of fuels on nanostructure and luminescence properties", *Ceram. Int.*, **43** (2017) 11469–11473.
17. M. Kabira, M. Ghahari, M.S. Afarani, "Co-precipitation synthesis of nano Y_2O_3:Eu^{3+} with different morphologies and its photoluminescence properties", *Ceram. Int.*, **40** (2014) 10877–10885.
18. Q. Pang, J. Shi, Y. Liu, D. Xing, M. Gong, N. Xu, "A novel approach for preparation of Y_2O_3:Eu^{3+} nanoparticles by microemulsion-microwave heating", *Mater. Sci. Eng. B*, **103** (2003) 57–61.
19. H. Yu, H. Wang, T. Li, R. Che, "Preparation and luminescent properties of YBO_3:Eu nanofibers by electrospinning", *Appl. Phys. A*, **108** (2012) 223–227.
20. A.B. Gawande, R.P. Sonekar, S.K. Omanwar, "Combustion synthesis and energy transfer mechanism of $Bi^{3+} \rightarrow Gd^{3+}$ and $Pr^{3+} \rightarrow Gd^{3+}$ in YBO_3", *Combustion Sci. Tech.*, **186** (2014) 785–791.
21. A. Nohara, S. Takeshita, Y. Iso, T. Isobe, "Solvothermal synthesis of YBO_3:Ce^{3+},Tb^{3+} nanophosphor: influence of B/(Y + Ce + Tb) ratio on particle size and photoluminescence intensity", *J. Mater. Sci.*, **51** (2015) 3311–3317.
22. D. Boyer, G. Bertrand, R. Mahiou, "A spectroscopic study of the vaterite form YBO_3:Eu^{3+} processed by sol-gel technique", *J. Lumin.*, **104** (2003) 229–237.
23. K. Park, S.W. Nam, "Enhanced photoluminescence of spray pyrolysis processed YBO_3:Eu^{3+} for PDP application", *Mater. Chem. Phys.*, **123** (2010) 360–362.
24. Y. Tian, B. Tian, B. Chen, C. Cui, P. Huang, L. Wang, R. Hua, "Ionic liquid-assisted hydrothermal synthesis and excitation wavelength-dependent luminescence of YBO_3:Eu^{3+} nano-/micro-crystals", *J. Alloys Compd.*, **590** (2014) 61–67.
25. S.M. Rafiaei, A. Kim, M. Shokouhimehr, "Effect of solvent on nanostructure and luminescence properties of combustion synthesized Eu^{3+} doped yttria", *Nanosci. Nanotech. Lett.*, **6** (2014) 692–696.
26. T. Verma, S. Agrawal, "Photoluminescent and thermoluminescent studies of Dy^{3+} and Eu^{3+} doped Y_2O_3 phosphors", *J. Fluores.*, **28** (2018) 453–464.
27. S.M. Rafiaei, A. Bahrami, "The effects of boric acid on crystal structure, nano/microstructure and photoluminescence characteristics of rare earth doped Y_2O_3/YBO_3 composite compounds", *J. Nanostruct. Chem.*, **7** (2017) 367–373.
28. L. Liu, R.J. Xie, C. Zhang, N. Hirosaki, "Role of fluxes in optimizing the optical properties of $Sr_{0.95}Si_2O_2N_2$:$0.05Eu^{2+}$ green-emitting phosphor", *Materials*, **6** (2013) 2862–2872.